

Consistent past half-century trends in the atmosphere, the sea ice and the ocean at high southern latitudes

Hugues Goosse · Wouter Lefebvre ·
Anne de Montety · Elisabeth Crespin ·
Alejandro H. Orsi

Received: 4 June 2008 / Accepted: 19 November 2008 / Published online: 3 December 2008
© Springer-Verlag 2008

Abstract Simulations performed with the climate model LOVECLIM, aided with a simple data assimilation technique that forces a close matching of simulated and observed surface temperature variations, are able to reasonably reproduce the observed changes in the lower atmosphere, sea ice and ocean during the second half of the twentieth century. Although the simulated ice area slightly increases over the period 1980–2000, in agreement with observations, it decreases by 0.5×10^6 km² between early 1960s and early 1980s. No direct and reliable sea ice observations are available to firmly confirm this simulated decrease, but it is consistent with the data used to constrain model evolution as well as with additional independent data in both the atmosphere and the ocean. The simulated reduction of the ice area between the early 1960s and early 1980s is similar to the one simulated over that period as a response to the increase in greenhouse gas concentrations in the atmosphere while the increase in ice area over the last decades of the twentieth century is likely due to changes in atmospheric circulation. However, the exact contribution of external forcing and internal variability in the recent changes cannot be precisely estimated from our results. Our simulations also reproduce the observed

oceanic subsurface warming north of the continental shelf of the Ross Sea and the salinity decrease on the Ross Sea continental shelf. Parts of those changes are likely related to the response of the system to the external forcing. Modifications in the wind pattern, influencing the ice production/melting rates, also play a role in the simulated surface salinity decrease.

1 Introduction

Over the period for which we have consistent satellite records, i.e., since November 1978, the sea ice extent and the sea ice area in the Southern Ocean have slightly increased (e.g. Zwally et al. 2002; Lemke et al. 2007; Comiso and Nishio 2008). One of the most recent estimates provides a weak positive trend of $0.9 \pm 0.2\%$ per decade for the ice extent and $1.7 \pm 0.3\%$ per decade for the sea ice area over the years 1978–2006 (Comiso and Nishio 2008). This clearly contrasts with the Northern hemisphere where the ice extent and ice area have decreased over the same period by $3.4 \pm 0.2\%$ and $4.0 \pm 0.2\%$ per decade, respectively (Comiso and Nishio 2008). An important question is to determine if those weak positive trends in the Southern Ocean are representative for the twentieth century or if a different behaviour was observed before the 1970s. To illustrate this point, indirect estimates of the location of the ice edge have been derived, mainly from whaling records and from the composition of ice cores drilled in Antarctica (e.g. de la Mare 1997; Curran et al. 2003; Cotté and Guinet 2007; de la Mare 2008). They suggest a significant decrease of the ice extent between the 1950s and the 1980s. However, the interpretation of these data is not straightforward and is still debated (e.g. Ackley et al. 2003;

H. Goosse (✉) · W. Lefebvre · A. de Montety · E. Crespin
Institut d'Astronomie et de Géophysique G. Lemaître,
Université Catholique de Louvain, Chemin du Cyclotron,
2, 1348, Louvain-la-Neuve, Belgium
e-mail: hugues.goosse@uclouvain.be; hgs@astr.ucl.ac.be

A. H. Orsi
Department of Oceanography, Texas A&M University,
College Station, TX, USA

W. Lefebvre
The Vlaams Instituut voor Technologisch Onderzoek (VITO),
Boeretang 200, Mol, Belgium

Cotté and Guinet 2007; Abram et al. 2007). This has led to the conclusion in the latest report of the Intergovernmental Panel on Climate Change (IPCC) that “the Antarctic data provide evidence of a decline in sea ice extent in some regions, but there are insufficient data to draw firm conclusions about hemispheric changes prior to the satellite era” (Lemke et al. 2007).

In the ocean, a clear warming signal has been observed in the latitude band 45–60°S since the 1950s at depths between 700 and 1,100 m (Gille 2002). This temperature increase is well reproduced by climate models if they include the forcing due to the changes in greenhouse gas concentrations in the atmosphere as well as the influence of the anthropogenic sulphate and volcanic aerosols (Fyfe 2006). At higher latitudes, observations are scarcer. Nevertheless, they suggest a warming at depths between 300 and 500 m, a surface freshening as well as a salinity decrease of bottom waters, at least in some regions (e.g. Robertson et al. 2002; Jacobs et al. 2002; Aoki et al. 2005a, b; Smedsrud 2005; Rintoul 2007).

A larger number of investigations has been devoted to assessing changes in the atmospheric temperature and circulation (e.g. Comiso 2000; Marshall 2003; Thompson and Solomon 2002; Turner et al. 2005; Chapman and Walsh 2007; Marshall et al. 2006, 2007; Monaghan et al. 2008; Steig et al. 2008). One of the clearest features detected is the large warming over the Antarctic Peninsula, with a temperature increase of more than 2.5°C over the last 50 years at some stations (Vaughan et al. 2003; Turner et al. 2005; Marshall et al. 2006, 2007). Although uncertainties are large in areas without station data, the temperature trends over most of the other regions of the continent appear generally positive for the period 1960–2005, but they are often insignificant. By contrast, negative trends are generally obtained for the period 1970–2005 (Chapman and Walsh 2007; Monaghan et al. 2008). Parts of those temperature changes have been related to the increase in the intensity of the southern annual mode (SAM) index over the last 30 years (e.g. Thompson and Solomon 2002; Marshall 2003; Turner et al. 2005; Marshall et al. 2006, 2007; van Lipzig et al. 2008). The SAM, which is the dominant mode of variability of the atmospheric circulation in the extratropics of the southern hemisphere, is related to a vacillation of the atmospheric mass (and thus of sea level pressure) between high and mid latitudes. An increase in the SAM index corresponds to an intensification and a southward shift of the westerlies over the Southern Ocean. As a consequence, a positive SAM index induces a stronger flow of relatively warm air of oceanic origin towards the Antarctic Peninsula which, in combination of a foehn effect on the eastern side of the Peninsula (Marshall et al. 2006), leads to a large warming over this part of the Antarctic continent. However, the

SAM alone could not explain the observed temperature changes there. A decrease in the sea ice extent and an overall increase in more northerly winds in this region must also play a role (e.g. Vaughan et al. 2003; Turner et al. 2005; Meredith and King 2005). In addition, a higher SAM index is associated with a larger isolation of the Antarctic continent (Thompson and Solomon 2002), i.e., weaker exchanges with lower latitudes, and thus a cooling compatible with the observed temperature decrease at many locations on the continent over the last 30 years.

Despite the recent studies of the influence of the changes in atmospheric circulation on the sea ice-ocean system (e.g. Lefebvre et al. 2004; Fyfe and Saenko 2006; Sen Gupta and England 2006; Ciasto and Thompson 2007; Stammerjohn et al. 2008; Yuan and Li 2008), we are still far from being able to determine which of the modifications observed in the atmosphere, the sea ice and the ocean are linked. Furthermore, we do not understand precisely the mechanisms which are responsible for those changes. For instance, we have not resolved the potential relationship between trends in surface air temperature over Antarctica and sea ice over the Southern Ocean. Our goal here is to study those potential links between the observed changes, providing a first step towards a more global understanding of the climate system at high southern latitudes. We also want to take advantage of those relationships to gain additional information on the elements of the system that are poorly constrained by long term observations, in particular the sea ice area.

To do so, we have performed a group of simulations with the climate model LOVECLIM, which includes fully coupled atmospheric, oceanic and sea ice components, using a simple data assimilation technique. The data used to constrain the model evolution are observations of near surface temperature at high southern latitudes over the period 1850–2000. Because of the small amount of data available and of the coarse resolution of the model, only the large-scale patterns could be reasonably analysed. In addition, we focus our attention on the decadal scale changes, not on interannual variability. The model and the data assimilation technique are described in Sect. 2. In Sect. 3, the model results are compared with data obtained at high latitudes in order to show that the simulations are able to satisfactorily reproduce the major observed changes (in the atmosphere, sea ice and ocean) over the last decades. The causes of the changes, and implications for longer term trends are discussed in Sect. 4, followed by the conclusions.

2 Model description and experimental design

LOVECLIM is a three-dimensional Earth system model of intermediate complexity that includes representations of

the atmosphere, the ocean and sea ice, the land surface (including vegetation), the ice sheets and the carbon cycle. As the global carbon cycle and the ice-sheet climate interactions are not the subject of our study, the ice sheet and carbon cycle components are not activated here in order to restrict the computer time and memory requirements of our simulations. These models components will thus not be described here. The atmospheric component is ECBILT2 (Opsteegh et al. 1998), a T21, three-level quasi-geostrophic model. The oceanic component is CLIO3 (Goosse and Fichefet 1999), which is made up of an ocean general circulation model coupled to a comprehensive thermodynamic-dynamic sea ice model. Its horizontal resolution is 3° by 3° , and there are 20 levels in the ocean. ECBILT-CLIO is coupled to VECODE, a vegetation model that simulates the dynamics of two main terrestrial plant functional types, trees and grasses, as well as desert (Brovkin et al. 2002). Its resolution is the same as the one of ECBILT. More information about the model and a complete list of references is available at the following address: <http://www.astr.ucl.ac.be/index.php?page=LOVECLIM%40Description>.

Two versions of the model are used here: LOVECLIM1.0 (Driesschaert et al. 2007) and the more recent LOVECLIM1.1 (Goosse et al. 2007). Compared to LOVECLIM1.0, the main modifications in LOVECLIM1.1 are related to the improvement of the land surface scheme as well as to the inclusion of a different emissivity for the various surface types and of a less diffusive numerical scheme in the ocean (Goosse et al. 2007). For LOVECLIM1.0, the model set up is identical to the one used by Goosse et al. (2006), although the model was not yet called LOVECLIM at that time but ECBILT-CLIO-VECODE (i.e. from the name of the components activated here). For LOVECLIM1.1, the parameter sets are the same as in experiment E3 of Goosse et al. (2007).

Both model configurations provide a reasonable mean climate at high latitudes. In particular, the ice extent in the Southern Ocean, defined as the total oceanic area with an ice concentration of at least 15%, is in good agreement with observations. Averaged over the period 1980–2000, its minimum is equal to 5.3×10^6 km² in LOVECLIM1.0 and 3.9×10^6 km² in LOVECLIM1.1 while the maxima for the same period are 18.4 and 17.8×10^6 km², respectively. Those values are close to the observed ones of 4.9 and 19.4×10^6 km² (Rayner et al. 2003). From this small difference between model and observations, LOVECLIM would be ranked amongst the best atmosphere ocean general circulation models (AOGCMs) regarding its ability to simulate the mean ice extent (Arzel et al. 2006). For the sea ice area, which is defined as the total surface covered by sea ice (i.e., excluding open water), the mean range of the seasonal cycle is 3.9 – 16.3×10^6 km² for LOVECLIM1.0

and 2.8 – 15.8×10^6 km² for LOVECLIM1.1. This is also close to the observed value of 3.1 – 16.1×10^6 km² (Rayner et al. 2003).

The two model configurations have a distinctly different response to a perturbation. For instance, the climate sensitivity (defined here as the global surface temperature change after 1,000 years in an experiment performed with LOVECLIM in which the CO₂ concentration increases from pre-industrial levels by 1% per year and is maintained constant after 70 years of integration when it reaches a value equal to two times the pre-industrial level) is 1.8°C in LOVECLIM1.0 and 2.8°C in LOVECLIM1.1 with the parameter values selected here. This is due to much stronger radiative feedbacks in LOVECLIM1.1 than in LOVECLIM1.0 (for more details on the parameters selection, see Goosse et al. 2007). Using both model versions could thus provide a test of the robustness of our results and of their dependence on the model behaviour.

The experiments analysed here cover the period 1851–2000. They are driven by natural (solar and volcanic) and anthropogenic (greenhouse gas, sulphate aerosols, land use) forcings, as described in Goosse et al. (2006). The initial conditions are derived from a numerical experiment covering the years 1–1850 AD using the same forcing, in order to take into account the long memory of the Southern Ocean (Goosse and Renssen 2005). For the 1851–2000 simulations, the model is forced to follow the observations of surface temperature, using an updated version of the data assimilation technique described in Goosse et al. (2006) (see also Collins 2003). The method is briefly described as follows. For the first year (1851 AD), a large ensemble of initial conditions (96 here) is generated by introducing very small perturbations in the quasi-geostrophic potential vorticity field. A 1 year simulation is then performed from all those initial conditions, forming a 96-member ensemble which provides a reasonable sample of model internal variability. The 96 simulations are then compared to the available observations for the corresponding year, using a cost function CF :

$$CF_k(t) = \sqrt{\sum_{i=1}^n w_i (F_{\text{obs}}(t) - F_{\text{mod}}^k(t))^2} \quad (1)$$

where $CF_k(t)$ is the value of the CF for each experiment k , for a particular period t ; n is the number of observations used in the model/data comparison. F_{obs} is the observed value of the variable F and F_{mod}^k is the value of F simulated in model experiment k at the same location. w_i is a weight factor. The member of the ensemble that is the closest to the observations, i.e., the one that minimises the CF, is selected as representative for this particular year. The state obtained at the end of the year in this simulation is then used as the initial condition for the subsequent year.

Finally, the procedure is repeated until year 2000 is reached.

By grouping all the years for which the agreement between model variability and the observed one is the best, we obtain a nearly continuous reconstruction for the period 1850–2000 (continuous if we neglect the small perturbation imposed on the quasi-geostrophic geopotential each first of January). This reconstruction is consistent with the forcing applied, the model physics, as well as with the observations used to constrain the model evolution, if the technique is successful.

The observations used here are annual mean near surface temperature at mid and high southern latitudes derived from the HADCRUT3 dataset over the period 1851–2000 (Brohan et al. 2006). Unfortunately, only a few observations are available for Antarctica and the surrounding seas, which are the main focus on our study (Fig. 1). In order to give a larger weight to those points, the region southward of 30°S has been first divided into seven boxes: an “Antarctic” box covering all the longitudes southward of 67°S, three boxes in the latitude band 50–67°S, corresponding to the “Ross” sector (135°E–85°W), the “Weddell” sector (85°W–0°E), and the “Amery” sector (0°E–135°E), and three boxes in the latitude band 30°S–50°S separated by the same longitudes. The surface temperature is first averaged over those boxes for both the observations and model results using in the latter case only the locations where observations are available. The CF is then evaluated by using those seven averages, so n equals 7 in Eq. 1 above. As a consequence, if the same weights are used for all the boxes, the few observations southward of 67°S have the same influence on the selection of the best simulation as the larger number of observations in a box between 30°S and 50°S.

For both model versions, three different experiments were launched. One with all the weights w_i equal to 1, one with the w_i for the four southernmost boxes equal to 1 and equal to 0.75 for the three northernmost boxes and one with the w_i for the four southernmost box equal to 1 and equal to 0.5 for the three northernmost boxes. The scatter between those six experiments, measured by the standard deviation of those six members, is used to estimate the uncertainty of our results. In particular, it allows determining if the model evolution is really constrained by the data or if small modifications in the design of the technique have a large influence.

3 Description of the changes

3.1 The surface and the atmosphere

As expected, in the six simulations using data assimilation, the simulated surface air temperature at high southern

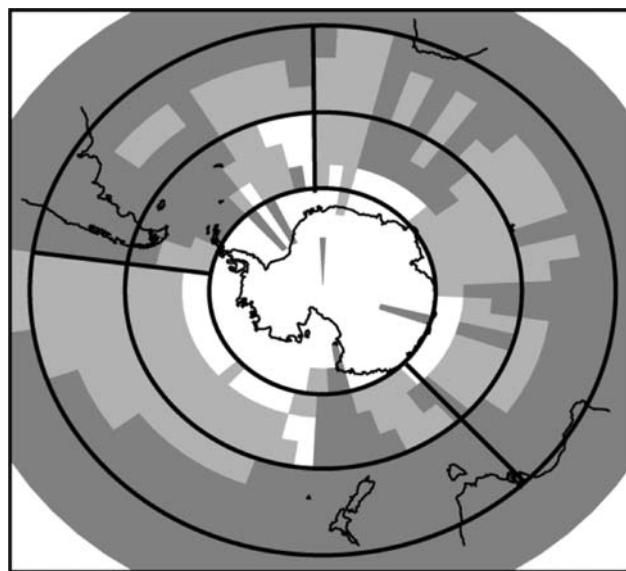
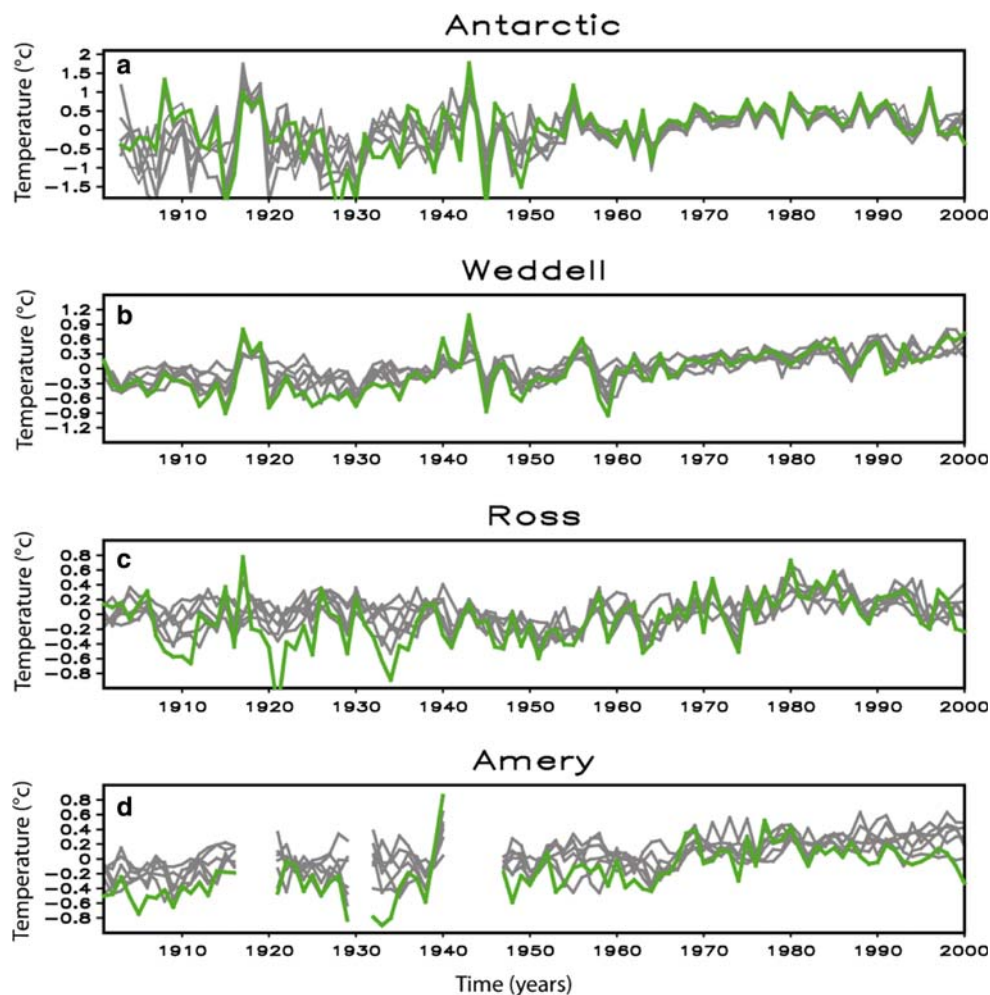


Fig. 1 The boundaries of the seven boxes used to compute the CF. The *dark grey area* represents the model grid boxes for which observations (Brohan et al. 2006) are available since 1960 while the *light grey area* represents the model grid boxes for which observations are available since 1980. No data is available in the *white grid boxes*

latitudes is very close to the observations used to constrain the model evolution (Fig. 2). The agreement is very high for the second half of the twentieth century, except maybe in the “Amery” sector where the model tends to overestimate the temperature over the last two decades. For the first half of the century, a larger variance is obtained for the temperatures averaged over the various boxes because of the smaller number of stations available. During this data-sparse period, the model simulates generally the same long term trend as the data but it fails to reproduce some of the largest anomalies such as the large cooling in 1922 in the “Ross” sector.

The spatial distribution of the simulated trend of the near-surface temperature over the Antarctic continent is also in relatively good agreement with recent estimates based on observations. Over the period 1960–2000 (Fig. 3 left column), the largest warming is found over the Antarctic Peninsula with values larger than 0.4°C per decade in both the model and the reconstruction of Chapman and Walsh (2007). Compared to the Peninsula region, a much weaker warming is simulated over the majority of the continent while a cooling is obtained only over the ocean, except for a very small zone close to the Ross Sea. In the climatology of Chapman and Walsh (2007), the cooling trend over this period is restricted to the centre of the continent but still covers a larger region compared to model results. By contrast, Steig et al. (2008) argue that the warming over West Antarctica may have been underestimated by previous reconstructions

Fig. 2 Anomaly of near surface temperature over the twentieth century at high latitudes. The green line is the HADCRUT3 dataset (Brohan et al. 2006). The grey lines are the results of the six model simulations all using HADCRUT3 to constrain the model evolution but using slightly different weights for the various grid boxes (Fig. 1) in the assimilation procedure. **a** The “Antarctic” box corresponds to an average over all the longitudes southward of 67°S. For the three other boxes, the average has been performed over the latitudes 50–67°S and longitudes. **b** 135°E–85°W (“Ross”), **c** 85°W–0°E (“Weddell”) and **d** 0°E–135°E (“Amery”). Only the points where observations are available are taken into account in the average so the number of points increases with time and is even zero during the late 1910s, early 1930s and early 1940s for the “Amery” area



and show a clear warming in this region over the period 1957–2007.

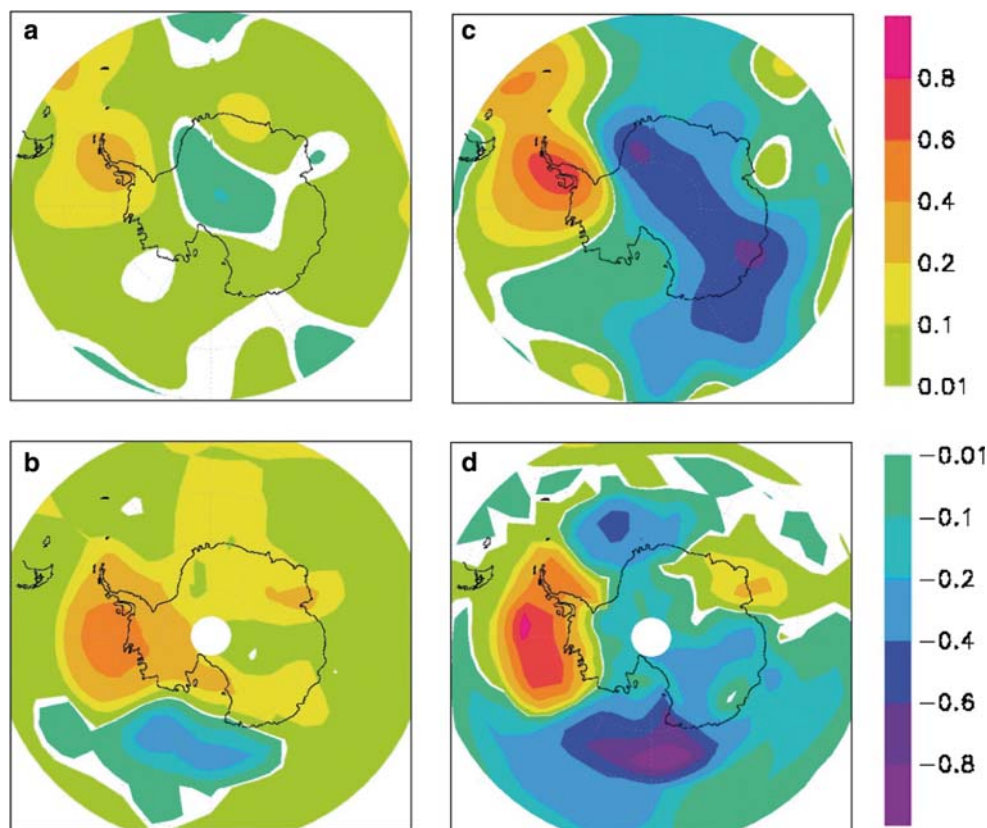
For the period 1980–2000 (Fig. 3 right column), in addition to a large warming being present mainly over the Antarctic Peninsula, a cooling over a large part of the continent is found both in model and observations. However, the cooling trend appears underestimated in our simulations. Chapman and Walsh (2007) argue that the uncertainty of their results is relatively large over the eastern continental interior where a large part of the discrepancies occurs. Nevertheless, it is reasonable to consider that the few data used to constrain model results in the continent interior (Fig. 1) are probably not sufficient to mitigate the externally forced climate trends that corresponds to a warming in those areas in LOVECLIM (Swingedouw et al. 2008, see also Sect. 4).

Compared to the dataset of Chapman and Walsh (2007), both positive and negative temperature trends are larger over the ocean in the simulations. Their analysis is based on various data sources, including direct surface temperature observations as in the HADCRUT3 dataset. However,

because of the data availability, land-based stations over Antarctica form the core of their analysis (see their Fig. 2) and uncertainties can be large over the ocean, in particular in the Amundsen Sea (see their Fig. 8). As the oceanic values of Chapman and Walsh (2007) are frequently extrapolations from land areas, this likely leads to smaller changes in their dataset than in our simulations for which the full model dynamics can induce large temperature variations over the ocean.

Different definitions have been proposed for the SAM index, all of them leading basically to the same conclusions. Here, for model results we apply a similar procedure as in Gong and Wang (1999) who define the SAM index as the difference between the zonal mean normalised sea level pressure between 40°S and 65°S. However, because sea level pressure is not a dynamic variable in our model (Opsteegh et al. 1998), we instead use the difference of normalised geopotential height at 800 hPa between the same latitudes. As the simulated atmospheric circulation is not directly constrained by the observations, the scatter between the different simulations is larger for the SAM

Fig. 3 Trend of annual mean near surface temperature over the period 1960–2000 for **a** the observations (Chapman and Walsh, 2007) and **b** for the model results averaged over the six simulations with data assimilation (units are K per decade). **c** and **d** are the trend for the period 1980–2000 for the observations and model results, respectively



index (Fig. 4) than for the surface temperature (Fig. 2). However, the standard deviation of the ensemble is still relatively low for the last 50 years and all the simulations show a clear increase of the SAM index between 1970 and 2000 consistent with observations. The decrease between 1950 and 1970 is also similar to the observed one. For the first half of the twentieth century, the range of the model results is larger, likely because of the smaller amount of temperature observations used to constrain model evolution. The long term increase obtained for the mean of the six simulations over this period bears clear similarities with a reconstruction of the SAM index in summer over the twentieth century (Jones and Widmann 2003, 2004) but the

uncertainties of model results are too large to gain robust conclusions for this period.

3.2 The sea ice

As found for the SAM index, the uncertainties in the simulated ice area are large for the first half of the twentieth century (Fig. 5). For the more recent past, the model simulations show clearly a decrease of about $0.5 \times 10^6 \text{ km}^2$ between the early 1960s and the early 1980s before a slight increase during the last 15 years. For comparison, this decrease centred over the 1970s corresponds to roughly half of the annual mean decrease

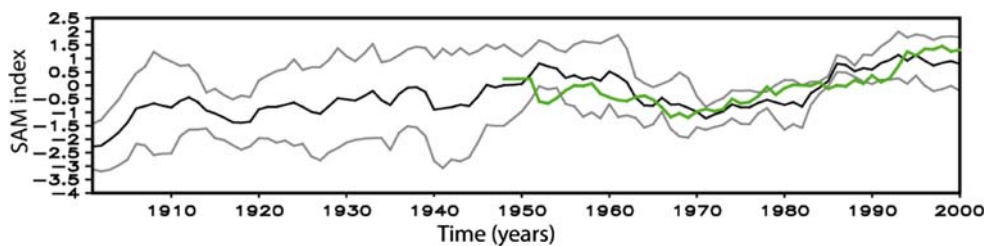


Fig. 4 Annual mean SAM index over the twentieth century. The *green curve* is the estimate of Marshall (2003), based on station data. The *black line* is the average over the six model simulations while the *grey lines* are the mean plus and minus one standard deviation of the ensemble. This standard deviation is computed for each time step. An

11-year running mean has been applied to the time series. Because of the different definitions of the SAM index, the model results have been scaled to have the same mean and variance as the observed index over the period 1960–2000

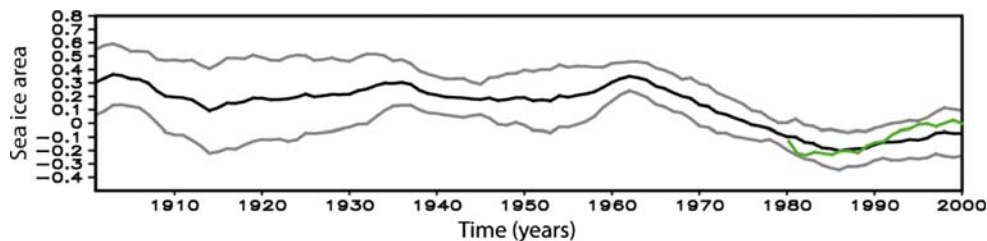


Fig. 5 Anomaly of annual mean sea-ice area (in 10^6 km^2) in the Southern Ocean over the twentieth century. The *green curve* is the estimate based on the HADISST data set (Rayner et al. 2003). The *black line* is the average over the six model simulations while the *grey*

lines are the mean plus and minus one standard deviation of the ensemble. An 11-year running mean has been applied to the time series. The reference period is 1960–2000

of the sea ice area in the Arctic over the last 30 years (e.g. Comiso and Nishio 2008).

Unfortunately, reliable continuous information on the sea ice concentration from satellite measurements is available only since November 1978. Over this period, the simulations are in good agreement with observations, both for the integral over the Southern Ocean (Fig. 5) as well as regionally (Fig. 6). In particular, the observed increase of the annual mean ice concentration in the Ross Sea and in the South Pacific, with values up to 0.1 per decade, is well reproduced by the model. Integrated over the whole Ross Sea (between 160°E and 140°W), the trend of the annual mean ice area over the period 1980–2000 reaches $0.15 \times 10^6 \text{ km}^2$ per decade for the mean of all the simulations compared to $0.17 \times 10^6 \text{ km}^2$ per decade in the observations (Rayner et al. 2003). In the Bellingshausen and Amundsen Seas, the model overestimates the ice extent compared to observation, leading to a too zonal ice edge (Fig. 6). As a consequence, the simulated decrease appears there a bit too diffuse. However, the trend over the period 1980–2000 integrated over both regions (140°W – 60°W), giving a value of $-0.08 \times 10^6 \text{ km}^2$ per decade, is also in good agreement with the observations of $-0.05 \times 10^6 \text{ km}^2$ per decade (Rayner et al. 2003). We must recall that our model has a relatively coarse resolution that does not allow reproducing all the regional details in currents and winds. Furthermore, no surface temperature observations are available in the Bellingshausen and Amundsen Seas to constrain the model evolution (Fig. 1). The good correspondence between simulated and observed ice concentration trends in this zone could thus be considered as a successful test of the ability of the method to provide reasonable results in regions without any data. This also increases our confidence in the value of the temperature trend simulated in this area (Fig. 3).

Before October 1978, no large scale data could be directly and quantitatively compared with model results. Early satellite observations obtained between December 1972 and March 1977 show a significantly higher ice extent over the early 1970s than during the last two decades

(e.g. Cavalieri et al. 2003). However, because of the absence of intercalibration with the other satellite sensors that have been operational after October 1978, these data are generally not included in the analysis of the recent trends (e.g. Lemke et al. 2007). It is the reason why they are not displayed on Fig. 5. Before this period, the information on the sea ice concentration is even sparser. The

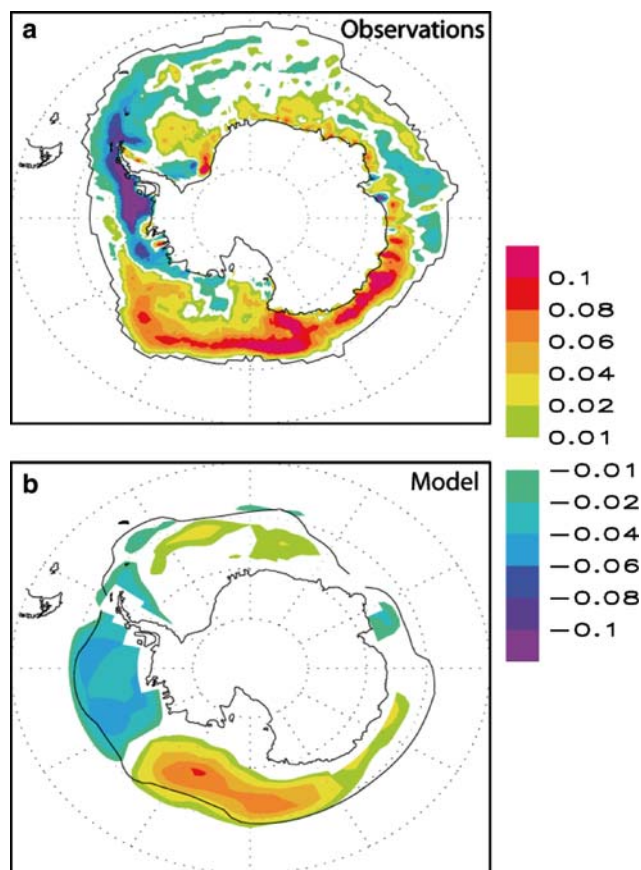


Fig. 6 The trend of annual mean sea-ice concentration over the period 1980–2000 for **a** the observations (Rayner et al. 2003) and **b** for the model results averaged over the 6 simulations with data assimilation (units are per decade). The *black line* represents the location of the September ice edge, as defined by an annual ice concentration equal to 15%, for the observation (**a**) and the model (**b**)

only nearly-continuous record for the twentieth century is, to our knowledge, the duration of fast ice record in the South Orkney Islands (northwest of the Weddell Sea, Murphy et al. 1995). It shows a decline during the 1950s and the 1960s which is preceded and followed by relatively stable conditions. For the HADISST dataset, prior to 1973, the ice edge location is based on two atlas climatologies: a climatology for the period 1929–1939, used to define the sea ice over the period 1871–1939, and a climatology based on information collected between 1947 and 1962 from Russian expeditions. For the period 1947–1962, this provides an ice area that is $0.4 \times 10^6 \text{ km}^2$ higher than over the last two decades while for the earlier period the ice area is higher by more than $1 \times 10^6 \text{ km}^2$. However, we must take into account that the uncertainties of the observation are very high for this period. For instance, analysing historical records of UK cruises from the 1920s and the 1930s, Ackley et al. (2003) suggested little change in the summer ice extent between the first half of the twentieth century and the years 1979–1998. Furthermore, the definition of the ice edge derived from ships, as used in those climatologies, can be very different from the one derived from satellite data. The bias on the ice extent between those two methods might reach more than $1 \times 10^6 \text{ km}^2$ during some seasons (e.g. Ozsoy-Cicek et al. 2008). As a detailed intercalibration is not presently available, this forbids a precise analysis of the long term trend in records such as HADISST which blends information from satellites and ship records.

Additional information on the sea ice cover could also be gained from indirect sources. Two such sources have received significant attention recently: the long-term whaling database and the methanesulfonic acid (MSA) measured in Antarctic ice cores. On the one hand, whales tend to feed close to the ice edge because of generally high zooplankton densities found there. The southernmost whale catches have thus been used as a proxy for the location of the ice edge (de la Mare 1997; Cotté and Guinet 2007; de la Mare 2008). On the other hand, MSA sources are ultimately related to marine phytoplankton productivity. As this productivity is strongly modified by sea ice processes at the ice margin, MSA has also been proposed as a proxy of the ice extent. These proxies are both difficult to interpret, and their ability to quantitatively estimate sea ice extent changes has been questioned (e.g. Ackley et al. 2003; Ozsoy-Cicek et al. 2008). In particular, the definition of the ice edge from the whaling record could be different from the one derived from satellite data, leading to a potential bias in the evaluation of long-term changes (e.g. Ackley et al. 2003; Cotté and Guinet 2007). Different types of whales could also feed at different distances from the ice edge (e.g. Cotté and Guinet 2007). For the MSA, a positive correlation with winter ice extent in the South Pacific

sector has been found for the Law Dome ice core (Curran et al. 2003) while a negative correlation has been obtained for the Weddell Sea, emphasising a cautious approach when using MSA data to reconstruct past circumpolar sea-ice changes (Abram et al. 2007). Despite large differences on the magnitude of the changes, the reconstructions based on those proxies all suggest a retreat of the ice cover since 1950 (de la Mare 1997; Curran et al. 2003; Cotté and Guinet 2007; de la Mare 2008). However, because of the uncertainties associated with those records, this result must be taken with great caution.

3.3 The ocean

In a few regions south of 60°S , it is possible to compare oceanic observations (starting in the 1950s) to model simulations for both the evaluation and investigation of simulated ocean changes. The Ross Sea continental shelf is probably the best-sampled shelf region in Antarctica, both in space and time, (e.g. Jacobs et al. 2002; Orsi and Wiederwohl 2008). Here, Jacobs et al. (2002) have shown a freshening at all depths over the continental shelf of the Ross Sea as well as a warming at intermediate depth (around 300 m) north of the continental shelf. By comparing the observations of Jacobs et al. (2002) with the result of an ocean-sea ice model, Assmann and Timmermann (2005) have suggested that in some regions, below 300 m, at least part of this trend could be due to aliasing irregularly sampled observations. Nonetheless, a comprehensive compilation of the Ross Sea hydrography (Stover 2006; Orsi and Wiederwohl 2008) confirms the widespread freshening observed during the past few decades over the Ross continental shelf, as reported by Jacobs et al. (2002). This is in qualitative agreement with our model results which give a near surface salinity decrease of about 0.04 psu on average over the entire Ross Sea continental shelf between 1960 and 2000 (Fig. 7). At the surface, the maximum freshening occurs actually in our simulations in the Amundsen Sea (Fig. 8). This is the region that Jacobs et al. (2002) proposed as the likely source for the anomalies observed in the Ross Sea, but observations are lacking to confirm this hypothesis. At depth, the freshening is detectable only on the shelf of the Ross Sea and Adélie Land because of the intense vertical mixing that induces a downward propagation of the signal. There, the salinity decrease could still be found close to the bottom (Fig. 9).

The amplitude of these simulated decadal changes in Ross Sea waters is smaller than the one reported by Jacobs et al. (2002) who show a decrease of ~ 0.1 psu near the western end of the Ross Ice Shelf, and by Stover (2006) who shows a freshening between 0.05 and 0.2 psu depending on the region analysed. The same conclusion is valid for the temperature north of the shelf. It is clearly

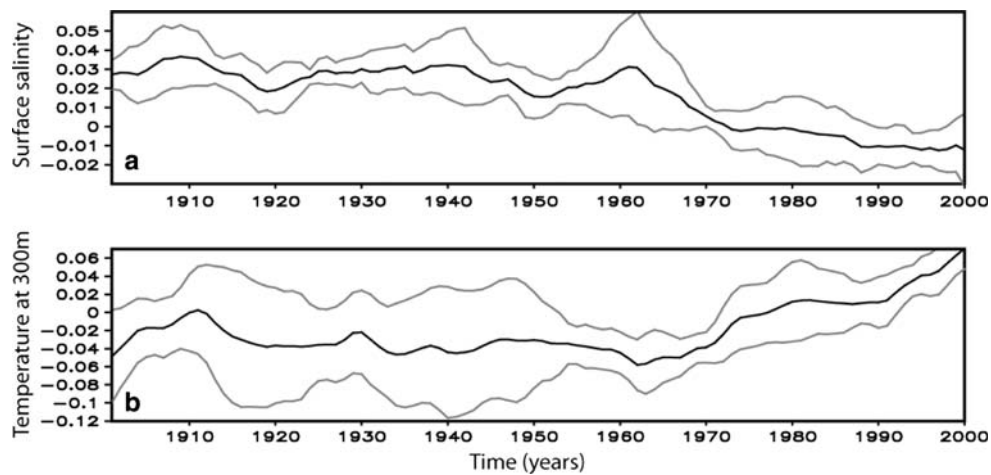


Fig. 7 **a** Surface salinity anomaly (in psu) averaged over the continental shelf of the Ross Sea (region shallower than 900 m in the area 170–200°E, 73.5–79.5°S) and **b** Ocean temperature anomaly in °C at a depth of 300 m averaged over the region north of the continental shelf of the Ross Sea (region deeper than 900 m in the

area 170–200°E, 67.5–73.5°S). The *black line* is the average over the six model simulations while the *grey lines* are the mean plus and minus one standard deviation of the ensemble. An 11-year running mean has been applied to the time series. The reference period is 1960–2000

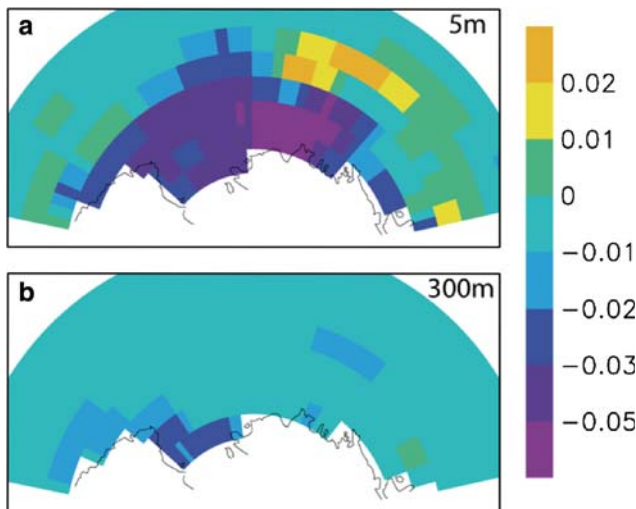


Fig. 8 Difference of ocean salinity (in psu) between 1980 and 2000 and 1950–1970 at **(a)** 5 m and **(b)** 300 m in the area 140–290°E, 58–80°S

increasing in the model but the warming is of 0.1°C at 300 m over the period 1960–2000 (Fig. 7). This is about half that estimated by Jacobs et al. (2002) and by Stover (2006). At deeper levels, a warming is also simulated north of the Ross Sea shelf but the amplitude decreases with depth, reaching 0.05°C in 40 years at 1,800 m.

The observations close to the continental slope, southward of 56°S, indicate a freshening of the bottom waters of the Australian Antarctic basin (between 80° and 150°E) since the late 1960s, with differences between a few thousands of psu up to 0.02 psu over this period (Whitworth 2002; Aoki et al. 2005b; Rintoul 2007). This is again in agreement with model results which display a

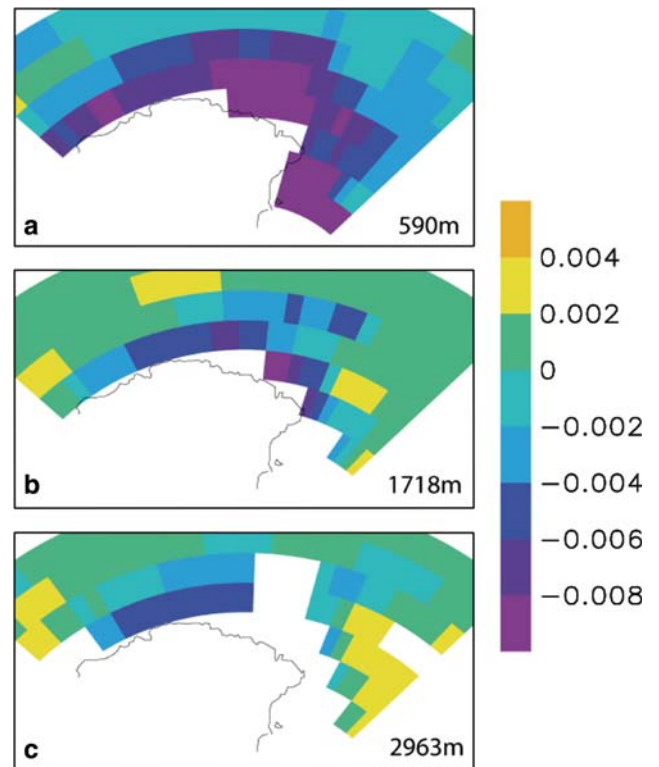


Fig. 9 Difference of ocean salinity (in psu) between the years 1980–2000 and 1950–1970 at **(a)** 590 m, **(b)** 1,718 m and **(c)** 2,963 m in the area 110–195°E, 58–80°S showing the propagation to great depth of the fresh anomaly originating from the continental shelf of the Ross Sea and Adélie Land

corresponding salinity decrease of about 0.005 psu. It has been suggested that this freshening is related to the salinity decrease in the zone of deep water formation (Aoki et al. 2005a, b; Rintoul 2007). This is perfectly consistent with

our simulations showing clearly the freshening signal cascading along the continental slope from the continental shelves of the Ross Sea and Adélie Land towards the ocean bottom (Fig. 9). In our simulations, the freshening is accompanied by a slight warming in this region.

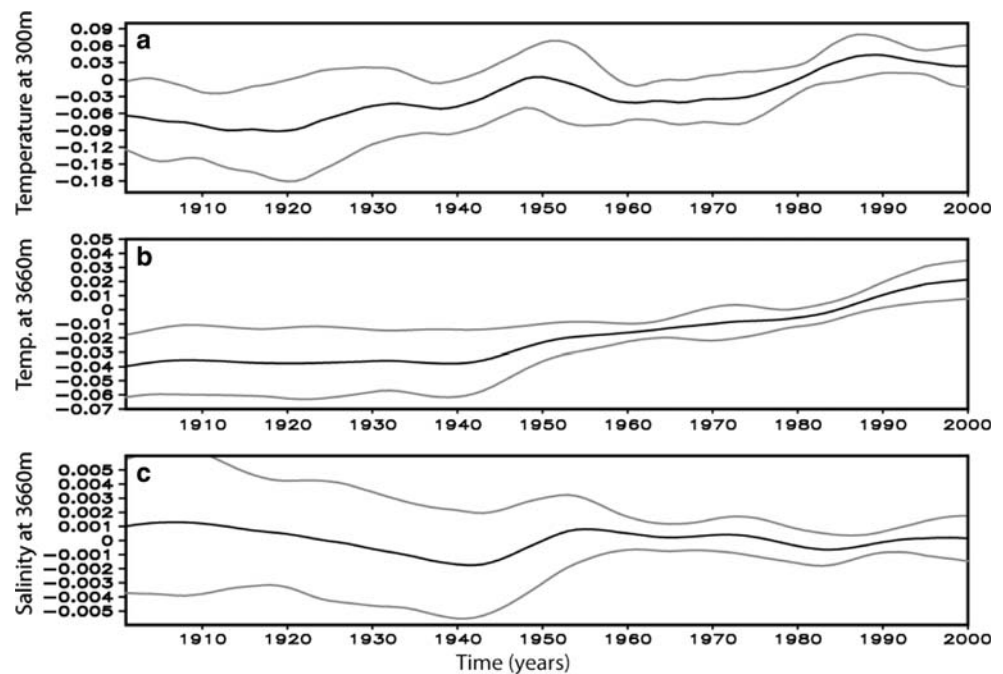
At a depth of 300 m, the simulations show in the Weddell Sea a long term warming (Fig. 10) as in the Ross Sea. This is qualitatively consistent with observations (e.g. Robertson et al. 2002). However, the magnitude of the trend is smaller and the decadal variability is larger in the Weddell Sea. There is even a small cooling over the last few years of the twentieth century, as observed by Fahrbach et al. (2004). Close to the bottom, the warming trend over the period 1950–2000 is slightly clearer than in the upper part of the water column (Fig. 10). Over the 1990s, the simulated warming rate reaches 0.001°C per year there, which is nearly identical to the one measured over the period 1992–1998 by Fahrbach et al. (2004). Fahrbach et al. (2004) mentioned that the trend has weakened and even reversed after 1998. We also simulate a weakening of the trend but a cooling during the last years of the twentieth century is only found above 2,500 m in the model (though it is propagating slowly downward).

In contrast to the Ross Sea, no clear freshening is simulated in the Weddell Sea over the last decades neither at the surface over the shelves nor in the deep ocean (Fig. 10). Some long term changes are noticed in the simulation but they vary strongly with depth and location. Consistent with model, Fahrbach et al. (2004) measured very small salinity variations over the 1990s. In contrast, Gordon (1998), in explaining water mass distribution measured in 1992,

postulated that the recently formed deep water appeared fresher. Such a freshening is not present in our model results.

An important feature of the Weddell Sea was the formation of the big Weddell Polynya in 1974, 1975 and 1976 (e.g. Carsey 1980). During those 3 years, a region covering about $0.25 \times 10^6 \text{ km}^2$ within the seasonal ice pack remained ice free all year long. The Weddell Polynya was associated with deep mixing in the ocean, bringing relatively warm and salty deep water to the surface (Gordon 1978, 1982). The resulting heat flux was high enough to compensate for the large sensible heat loss towards the atmosphere during winter without significant ice formation. This intense vertical mixing has profoundly modified the characteristics of the water masses in this region, affecting the system on decadal scales at least (Gordon 1982; Smedsrud 2005; Fahrbach et al. 2006; Gordon et al. 2007). Part of the oceanic trends observed since 1977 may thus be attributed to a recovery from those events. Unfortunately, the data constraints used in our numerical experiments appear too weak to force the model to simulate a large polynya in the Weddell Sea. The model displays clear variations in the intensity of vertical mixing in this region. In particular, relatively strong mixing is simulated in the 1970s as well as in the 1950s, the absolute maximum being in the 1930s. However, the coincidence could likely occur just by chance. Furthermore, this increase in vertical mixing is too weak to be considered as equivalent to the observed processes during the three years when the Weddell Polynya occurred. This must be kept in mind when analysing the model results in the Weddell Sea.

Fig. 10 (a) Temperature anomaly (in °C) at 300 m depth, (b) 3,660 m depth and (c) salinity anomaly (in psu) at 3,660 m depth averaged over the Weddell Sea (60°W–9°E, 64.5–79.5°S). The *black line* is the average over the six model simulations while the *grey lines* are the mean plus and minus one standard deviation of the ensemble. An 11-year running mean has been applied to the time series. The reference period is 1960–2000



4 Analysis of the causes of the changes

The description of our results in Sect. 3 has shown that our simulations using observed near surface temperature to constrain model evolution are able to reasonably reproduce the major observed trends over the last 50 years in the lower atmosphere, the sea ice and the ocean. Although the simulated signal in the ocean has the right sign, it appears somewhat weaker than the observed one. However, this could be due to the fact that we present averages over relatively large regions for the simulations (which are certainly the most robust features for a coarse resolution model) while observations come mainly from more restricted areas or circulation features not well resolved by the model. The changes in atmospheric circulation have been well described previously (e.g. Thompson and Solomon 2002; Gillett and Thompson 2003; Arblaster and Meehl 2006), so we mainly focus our attention on the ocean and sea ice here. In those two media, the decrease in sea ice area (Fig. 5), the freshening of the continental shelf of the Ross Sea as well as of the bottom water in the Australian Antarctic basin and the warming at mid-depth north of the continental shelf of the Ross Sea (Fig. 7) are probably amongst the clearest and most interesting modifications over the last 50 years. The goal of this section is to analyse the causes of those changes.

As a first step, we should determine if the observed trends are consistent with the response of the system to changes in the radiative forcing. In order to isolate this response, we use two ensembles of simulations. The first one consists of an ensemble of 20 numerical experiments performed with LOVECLIM driven by the same forcing as described in Sect. 2 but without data assimilation (10 simulations with LOVECLIM1.0 and 10 with LOVECLIM1.1 were used for consistency with the data assimilated runs although the two model versions give a similar response in the Southern Ocean). The second one is based on the simulations performed with AOGCMs for the Fourth Assessment Report of the Intergovernmental Panel on Climate Change (IPCC AR4). Here, the results of 16

GCMs are used: IPSL-CM4, CNRM-CM3, GISS-AOM, GISS-ER, CSIRO-Mk3.0, INM-CM3.0, UKMO-HadGEM1, UKMO-HadCM3, MRI-CGCM2.3.2, MIROC3.2 (hires), MIROC3.2 (medres), CGCM3.1 (T47), CGCM3.1 (T63), CCSM3, ECHAM5/MPI-OM, ECHO-G. Detailed information about the different models can be found at the website <http://www-pcmdi.llnl.gov/>. For both ensembles, the mean over all the members is displayed since the quasi-random internal variability tends to be filtered out by the averaging process, leaving only the forced component. Furthermore, for the IPCC simulations, the mean over all the models has proved to perform better than any individual model for a large range of diagnostics (e.g. Lefebvre and Goosse 2008a; Gleckler et al. 2008).

The sea ice area decrease between 1950 and 2000 in the simulation with data assimilation has a similar magnitude as the ensemble mean of the simulations performed using the AOGCMs and LOVECLIM without data assimilation over the same period (Fig. 11). Furthermore, when comparing the means over 1980–2000 and 1950–1970 in the simulation with data assimilation, the annual mean ice concentration decreases nearly everywhere (except in the Ross Sea) (Fig. 12). This pattern is very similar to the one resulting from an increase in greenhouse gas concentrations (see for instance Fig. 5c of Lefebvre and Goosse 2008a). As a consequence, the long term trend over the last 50 years of the twentieth century appears largely consistent with the modelled response to an increase in greenhouse gas concentrations. By contrast, if we restrict the analysis over the post 1979 period, the internal variability, as captured by the assimilation of surface temperature, strongly modulates the forced response of the model, resulting in the absence of a clear trend over this period. As already shown for surface temperature (see Fig. 3), this indicates that the trends over the last 21 years of the twentieth century for which we have reliable satellite information are likely not representative of the evolution of sea ice area over a longer period.

For the years 1910–1960, the ice area show mainly decadal variability in the simulation with data assimilation,

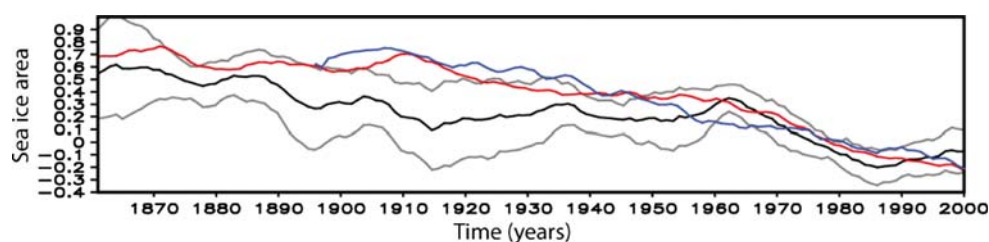


Fig. 11 Anomaly of annual mean sea-ice area (in 10^6 km^2) in the Southern Ocean. The *black line* is the average over the six model simulations while the *grey lines* are the mean plus and minus one standard deviation of the ensemble (same as Fig. 5). The *red line* is

the mean of an ensemble of 20 simulations made with LOVECLIM1.0 and LOVECLIM1.1 but without data assimilation. The *blue line* is the mean over 16 model simulations performed in the framework of the fourth IPCC report

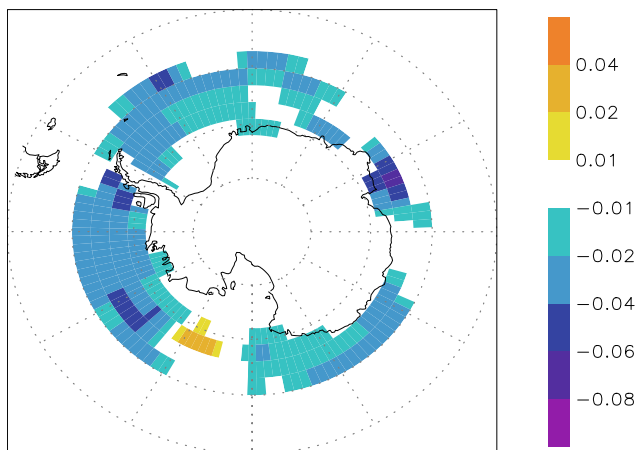


Fig. 12 Difference in annual mean sea ice concentration between the periods 1980–2000 and 1950–1970 averaged over the six LOVECLIM simulations with data assimilation

in contrast to the forced response that shows a monotonic decrease. This result must be taken with caution as the constraints are weak over this period and the uncertainties large. However, it nicely illustrates that internal variability could mask the forced response over relatively long periods for sea ice in the Southern Ocean and that the recent period for which the ice cover is relatively stable might not be exceptional in the context of the past century.

Over 1900–2000, the surface salinity decrease on the continental shelf of the Ross Sea and the subsurface temperature increase north of the shelf obtained in the simulation with data assimilation appear largely consistent with the forced response of the system (Fig. 13). This forced response displays of course some spatial variability but the changes

simulated in the Ross Sea have a magnitude similar to the ones simulated in many regions of the high latitudes of the Southern Hemisphere. Furthermore, according to the projections performed with AOGCMs, both the surface salinity decrease and the warming are expected to continue during the twenty first century (not shown).

The high latitude freshening in response to an increase in the atmospheric greenhouse gas concentration in the atmosphere has been classically attributed to an intensification of the freshwater cycle, leading to increased precipitation over the Southern Ocean (Sarmiento et al. 1998). Ice shelf melting as well as changes in ice production and transport could also play a role in this salinity decrease (Jacobs et al. 2002; Bitz et al. 2006). For the subsurface oceanic warming, it is an expected consequence of the higher radiative forcing resulting in a global temperature increase (e.g. Meehl et al. 2007). Furthermore, because of the surface freshening and of the subsurface to intermediate warming, the stratification increases in the Southern Ocean (e.g. Sarmiento et al. 1998; Bitz et al. 2006). This inhibits the vertical exchanges, leading to a decrease of the vertical heat fluxes (Fig. 14) from the relatively warm deeper levels to the colder surface and finally to an additional subsurface warming. Those arguments appear to be valid in our simulations.

The maximum in salinity changes found in the Amundsen Sea in our simulation with data assimilation (Fig. 8) is not a robust characteristic of the forced response of LOVECLIM and the AOGCMs (not shown). This feature appears rather related in the simulation with LOVECLIM using data assimilation to anomalous northerly winds that tend to transport more ice toward the coast

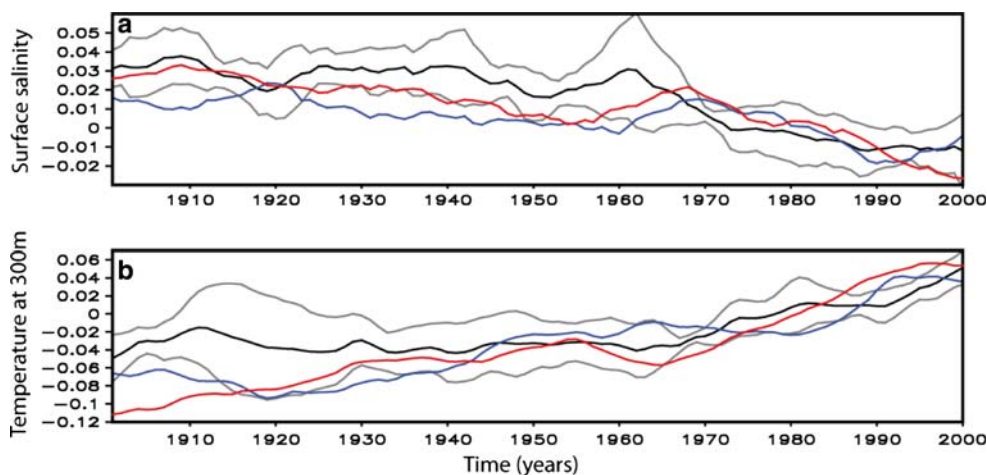


Fig. 13 **a** Surface salinity anomaly (in psu) averaged over the continental shelf of the Ross Sea (170–200°E, 73.5–79.5°S) and **b** Ocean temperature anomaly in °C at 300 m averaged over the region north of the continental shelf of the Ross Sea (170–200°E, 67.5–73.5°S). The black line is the averaged over the six model simulations while the grey lines are the mean plus and minus one

standard deviation of the ensemble (same as Fig. 7). The red line is the mean of an ensemble of 20 simulations made with LOVECLIM1.0 and LOVECLIM1.1 but without data assimilation. The blue line is the mean over 16 model simulations performed in the framework of the fourth IPCC report

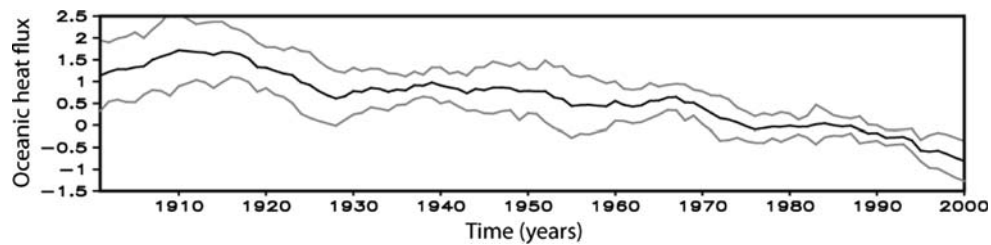


Fig. 14 Anomaly of the vertical heat flux at the ocean surface (in W m^{-2} , positive upward) averaged over the region south of 60°S . The *black line* is the averaged over the six LOVECLIM simulations with

data assimilation while the *grey lines* are the mean plus and minus one standard deviation of the ensemble. A 11-year running mean has been applied to the time series. The reference period is 1960–2000

in this area, leading to decrease in ice production and an increase in ice melting. The maximum difference in net ice production between 1950–1970 and 1980–2000 reaches more than 10 cm per year in this area. In addition, this anomalous southward ice transport is responsible for the salinity increase simulated further offshore (Fig. 8). Both Jacobs et al. (2002) and Assmann and Timmermann (2005) suggest that the salinity anomalies observed on the Ross Sea continental shelf could be traced upstream to the Amundsen Sea. Assmann and Timmermann (2005) advocate an important role of an upwelling in the Amundsen Sea in the generation of the anomalies there. The cyclonic wind pattern responsible for the anomalous ice transport mentioned above is also associated with a weak upwelling but it does not seem to play a large role in the salinity changes obtained in our simulations with data assimilation. In addition, Jacobs et al. (2002) consider that ice shelf melting could also be responsible for a significant part of the observed freshening. Melting of the ice shelves is taken into account in LOVECLIM (Beckmann and Goosse 2003) and the magnitude of this flux has increased in our simulation by nearly 10% over the twentieth century. However, because of the coarse model resolution, ice shelves are not represented between 115° and 150°W and the parameterization of Beckmann and Goosse (2003) injects the freshwater between 200 and 600 m, with only a moderate influence at the surface. This could explain why we tend to underestimate the observed surface freshening in the Ross Sea continental shelf region.

In contrast to Fig. 9, the freshening signal on the Ross Sea continental shelf does not propagate towards great depth during deep water formation in the simulation with AOGCMs and with LOVECLIM without data assimilation. This is due, in those simulations, to the mixing during the descent along the slope of the fresher shelf waters with saltier ambient deep water compared to the simulation with LOVECLIM using data assimilation. As a consequence the bottom salinity tends to increase in the mean of AOGCMs simulations during the twentieth century and this is projected to continue during the twenty first century (not shown). Following this analysis, the freshening of bottom

water in the Australian Antarctic sector found in both the observations and in LOVECLIM using data assimilation would not be attributed to a response to the forcing. However, the representation of processes associated with deep water formation is quite poor in global models, in particular the one of mixing during the descent along the slope. Furthermore, the results in the deep Southern Ocean vary strongly amongst the different AOGCMs. The mean over all of them could thus not be considered as providing a robust estimate of the forced response. It is then more reasonable to consider that, at this stage, the future evolution of bottom water properties close to the Antarctic continent is still an open issue.

The decrease in the upward heat flux in the Southern Ocean (Fig. 14) has been classically invoked to explain the weaker changes in surface temperature and sea ice area observed during the last decades at high southern latitudes compared to the ones noticed in the Arctic (e.g. Manabe et al. 1991; Gregory 2000; Goosse and Renssen 2001; Bitz et al. 2006; Zhang 2007). In agreement with those studies, the surface oceanic heat flux (positive upward) integrated over the whole area southward of 60°S decreases by more than 2 W m^{-2} over the twentieth century in our simulations with data assimilation. This decrease of the oceanic heat loss at high latitudes is larger in absolute value than the estimated increase of the global mean anthropogenic forcing over the same period (1.6 W m^{-2} following Forster et al. 2007) and thus has an important climatic role. However, as indicated by Fig. 14, the slope of the time evolution of the flux is roughly constant. As a consequence, it does not appear to be responsible for the simulated reversal from a decrease of the ice area between the early 1960s and early 1980s to an increase after 1985 (Fig. 5).

The cause of this change in the slope should then be looked for in the atmospheric circulation, in particular the increase in the SAM index since the early 1970s. As underlined in many studies the SAM has a large influence on regional sea ice anomalies during the various seasons (Liu et al. 2004; Lefebvre et al. 2004; Stammerjohn et al. 2008; Lefebvre and Goosse 2008a, see also Sect. 3.2). For the observed annual mean sea ice area, the correlation over

the period 1980–2000 with the observed annual mean SAM index is positive ($=0.31$ for detrended series). However, because of the short duration of the available time series, the correlation between the annual mean SAM index and the annual mean sea ice area is not significant at the 95% level (taking into account the reduced number of freedom caused by the detrending). Regionally, a positive SAM index is associated with a higher sea ice concentration in the Amundsen and Ross sectors while sea ice concentration tends to be lower in the Bellingshausen and Weddell Seas (see for instance Fig. 17 of Sen Gupta and England 2006 and Fig. 8 of Lefebvre and Goosse 2008a). This pattern, which bears clear similarities with the sea ice concentration trends over the last decades (Fig. 6), is mainly influenced by the fact that the SAM is not a perfectly annular mode (Lefebvre et al. 2004). Indeed, a low pressure system tends to develop over the Amundsen Sea when the SAM index is positive. It induces anomalous southerly winds over the Ross Sea that bring cold air to this region and push sea ice offshore, both effects leading to a higher ice area there. By contrast, the anomalous northerly winds over the Bellingshausen Sea are associated with a lower sea ice area.

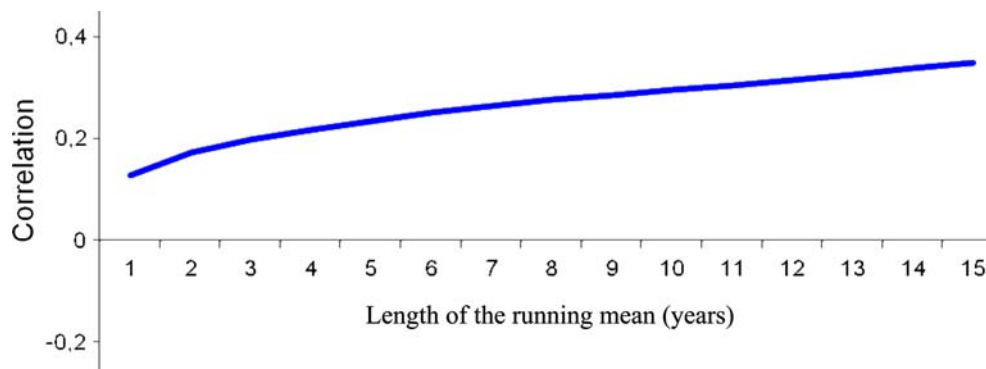
LOVECLIM, as well as the AOGCMs, tend to give lower correlations between the SAM index and the ice area than the observed one over the last decades. Nevertheless, as the latter value is not significant, this does not allow stating that our model underestimates the link between the SAM and the ice area integrated over the Southern Ocean. In LOVECLIM, the correlation for decadal scale variability is higher than the one related to interannual variability (Fig. 15). This leads us to the hypothesis that, for low frequencies, the cooling at high latitudes associated with the SAM (Thompson and Solomon 2002) outweighs the influence of the regional changes due to the meridional winds anomalies that governs the interannual variability (Lefebvre et al. 2004), leading to a larger ice area. Unfortunately, the scatter of the simulations covering the twentieth century using AOGCMs is so large that they could not be used to confirm or invalidate the results of

LOVECLIM. Despite those uncertainties, we can estimate that in LOVECLIM, using a 11-year running mean, a change in one standard deviation of the SAM is associated with a $0.11 \times 10^6 \text{ km}^2$ increase in ice extent. As in our simulations using data assimilation, the SAM has increased by more than 2 standard deviations between 1975 and 2000 (Fig. 4), this would correspond to an increase of $0.25 \times 10^6 \text{ km}^2$. Such a change could thus explain in our simulations a major part of the simulated increase in ice area over this period (Fig. 5).

Many studies have been recently devoted to the analysis of the causes of the increase in the SAM index that appears to have a large role in our simulations (e.g. Thompson and Solomon 2002; Gillett and Thompson 2003; Raphael and Holland 2005; Miller et al. 2006; Arblaster and Meehl 2006; Cai and Cowan 2007; Crook et al. 2008). In the GCMs used for the IPCC AR4, the models that contain a time variable stratospheric ozone forcing produce an average trend that is comparable to the observed one. Without such a stratospheric ozone forcing, the trend is still positive but weaker (e.g. Arblaster and Meehl 2006; Miller et al. 2006; Cai and Cowan 2007). This indicates that both the increase in greenhouse gas concentrations in the atmosphere and the stratospheric ozone depletion contributed to the increase in the SAM observed during the last 30 years, the ozone changes being likely the largest contributor. Nevertheless, the uncertainties on the amplitude of this forced response are still large. For instance, some studies suggest an underestimation of the coupling between stratospheric and surface changes in models that would lead to a too weak response of the atmospheric circulation to the increase in greenhouse gas concentrations in the atmosphere (e.g. Miller et al. 2006). In addition, the ozone changes applied for the AR4 might be too simple to capture the full response of the climate system to this forcing (e.g. Crook et al. 2008; Son et al. 2008).

Unfortunately, our results could not bring new information on this topic. Because of its low resolution and the absence of time variable ozone forcing, the forced trend in the SAM index over the last decades of the twentieth

Fig. 15 Correlation between the annual mean SAM index and the annual mean sea ice area in a 2,000 year simulation using LOVECLIM1.1 with constant forcing after applying a running mean of different lengths



century is relatively weak in LOVECLIM. It is thus likely that, in order to reproduce the observed trends (Fig. 4), the data assimilation technique compensates for an underestimation of the forced response by pushing the atmospheric circulation preferentially towards a state that is obtained in the real world as a response to the forcing. Unfortunately, we could not determine the magnitude of such a compensation as no reliable estimate of the forced response of the system is presently available. To do this, simulations with the highest possible resolution both in the vertical and horizontal, including the best possible physics (and probably chemistry, see for instance Son et al. 2008) and the most detailed forcing are required, providing results that would be perfectly complementary to the ones obtained here using data assimilation.

5 Conclusions

We have shown that the assimilation of surface temperature in a coupled climate model provides reasonable estimate of atmospheric, sea-ice and oceanic changes during the past half century, in agreement with the observed large-scale and long-term trends at high southern latitudes. For example, we are able to reproduce the small increase in ice area integrated over the Southern Ocean observed by satellites over 1979–2000. Prior to this small increase, our simulations show a decrease in Southern Ocean sea ice area of $0.5 \times 10^6 \text{ km}^2$ between the early 1960s and the early 1980s. It is intriguing that this decrease is in qualitative agreement with totally independent estimates based on whaling records and MSA measurements in an ice core (e.g. Cotté and Guinet 2007; Curran et al. 2003). However, the uncertainty of those proxy based reconstructions is too large to consider this agreement as a firm confirmation of the model results.

In the absence of such a confirmation, the decrease of sea ice extent obtained in our simulation with data assimilation could not be considered as a precise and definitive reconstruction of past sea ice changes before 1979. However, we provide results that are internally consistent for the atmosphere, ocean and sea ice, i.e., they respect all of the physical equations of the modelled system and are driven by reasonable estimates of past changes in external forcings. Our results are also able to reproduce reasonably well the observations of surface temperature changes that were used to constrain the model evolution as well as independent observations obtained in the atmosphere and the ocean over the last 50 years. The simulated sea ice trends obtained here can thus be said to be dynamically consistent with those observed variations in the atmosphere and ocean. In the absence of any results showing that it is not valid, it is thus reasonable to consider that the

simulated sea ice trends we have obtained provides a reasonable hypothesis about real past changes that could be further tested when new information will become available.

This conspicuous decrease in ice area obtained in our simulation with data assimilation is similar to the response over the last 50 years to the changes in external forcing as simulated by climate models. Considering that our reconstruction of past changes is a reasonable hypothesis leads us to a new interpretation of the ability of models to simulate the recent changes in ice area in the southern hemisphere. Up to now, the various studies analysing the model results in the Southern Ocean argue that models are generally not able to simulate the observed increase in ice extent and area since 1978 (Arzel et al. 2006; Parkinson et al. 2006; Lefebvre and Goosse 2008b). The modelled variability is usually large enough to consider that the observed evolution is still in the range provided by the simulations. Nevertheless, this is a somewhat weak conclusion on the model validity. By contrast, based on our hypothesis about past sea ice changes over a slightly longer period, we could now propose the alternative interpretation that the decrease of the ice area simulated by AOGCMs is perfectly consistent with our estimated retreat of the ice cover over the last 50 years.

The freshening in some areas of the Southern Ocean and the subsurface warming observed at many locations could also be interpreted as induced, at least partly, by changes in external forcing. Anomalies in the wind field and the associated modification in ice formation/melting rates are also responsible for important salinity changes in LOVECLIM using data assimilation. Those later processes appear to play an important role in our simulations in the Amundsen Sea, a region that is considered in several studies as the source of the observed freshening on the Ross Sea continental shelf. Because of the relatively poor representation of bottom water formation in global climate models, the causes of the observed freshening of bottom water in the Indian and Pacific Oceans are not yet clear. Nevertheless, they are probably related to the freshening observed on the Ross Sea shelf.

In our simulations, the increase in ice area integrated over the southern hemisphere since 1985 could reasonably be attributed to changes in the atmospheric circulation. In particular, the increase in the SAM index over the last 30 years likely plays an important role since, at decadal scale, a positive SAM index is clearly associated with a higher ice area in LOVECLIM. However, because of the uncertainties in the results of different models and the short duration of the observed time series, the influence of SAM on the ice-ocean system at decadal scale needs to be further investigated, in particular by looking at its role during the different seasons. Determining the exact causes of the changes over the last 50 years also needs additional

studies. Our results show that internal variability can mask over several decades the trends that would be induced by external forcing only, in particular for the sea ice area, but the respective role of internal variability and external forcing in past changes could not be estimated precisely from our analysis.

We have also shown that the observed changes in the Southern Ocean are the results of the delicate balance between several processes: thermodynamic response to the radiative forcing, changes in the intensity of the SAM, the oceanic stratification and the oceanic heat transport, modification of the sea-ice transport, etc. The net effect of all those elements on surface temperature, sea-ice extent or deep water formation is very likely different when studying different periods. Extrapolating the conclusions of our study for future or past conditions, by taking into account only one part of the relevant processes, should thus be considered as hazardous.

Acknowledgments H. Goosse is Research Associate with the Fonds National de la Recherche Scientifique (FNRS-Belgium). This work is supported by the FNRS and by the Belgian Federal Science Policy Office, Research Program on Science for a Sustainable Development. We would like to thank Marie-France Loutre for her help in the experimental design and Martin Vancoppenolle for a careful reading of the manuscript. We acknowledge the international modelling groups for providing their data for analysis, the Program for Climate Model Diagnosis and Intercomparison (PCMDI) for collecting and archiving the model data, the JSC/CLIVAR Working Group on Coupled Modelling (WGCM) and their Coupled Model Intercomparison Project (CMIP) and Climate Simulation Panel for organising the model data analysis activity, and the IPCC WGI TSU for technical support. The IPCC Data Archive at Lawrence Livermore National Laboratory is supported by the Office of Science, US Department of Energy. This work was initiated during the CLIVAR/CLIC/SCAR Southern Ocean Region Implementation Panel meeting held in Buenos Aires, 14–17 November 2006.

References

- Abram NJ, Mulvaney R, Wolff EW, Mudelsee M (2007) Ice core records as sea ice proxies: an evaluation from the Weddell Sea region of Antarctica. *J Geophys Res* 112:D15101. doi:[10.1029/2006JD008139](https://doi.org/10.1029/2006JD008139)
- Ackley S, Wadhams P, Comiso JC, Worby AP (2003) Decadal decrease of Antarctic sea ice extent inferred from whaling records revisited on the basis of historical and modern sea ice records. *Polar Res* 22(1):19–25. doi:[10.1111/j.1751-8369.2003.tb00091.x](https://doi.org/10.1111/j.1751-8369.2003.tb00091.x)
- Aoki S, Rintoul SR, Ushio S, Watanabe S, Bindoff NL (2005a) Freshening of the Adélie Land bottom water near 140°E. *Geophys Res Lett* 32:L23601. doi:[10.1029/2005GL024246](https://doi.org/10.1029/2005GL024246)
- Aoki S, Bindoff NL, Church JA (2005b) Interdecadal water mass changes in the Southern Ocean between 30°E and 160°E. *Geophys Res Lett* 32:L07607. doi:[10.1029/2004GL022220](https://doi.org/10.1029/2004GL022220)
- Arblaster JM, Meehl GA (2006) Contributions of external forcings to southern annular mode trends. *J Clim* 19(12):2896–2905. doi:[10.1175/JCLI3774.1](https://doi.org/10.1175/JCLI3774.1)
- Arzel O, Fichefet T, Goosse H (2006) Sea ice evolution over the 20th and 21st centuries as simulated by current AOGCM. *Ocean Model* 12:401–415. doi:[10.1016/j.ocemod.2005.08.002](https://doi.org/10.1016/j.ocemod.2005.08.002)
- Assmann KM, Timmermann R (2005) Variability of dense water formation in the Ross Sea. *Ocean Dyn* 55:68–87. doi:[10.1007/s10236-004-0106-7](https://doi.org/10.1007/s10236-004-0106-7)
- Beckmann A, Goosse H (2003) A parameterization of ice shelf-ocean interactions for climate models. *Ocean Model* 5(2):157–170. doi:[10.1016/S1463-5003\(02\)00019-7](https://doi.org/10.1016/S1463-5003(02)00019-7)
- Bitz CM, Gent PR, Woodgate RA, Holland MM, Lindsay R (2006) The influence of sea ice on ocean heat uptake in response to increasing CO₂. *J Clim* 19:2437–2450. doi:[10.1175/JCLI3756.1](https://doi.org/10.1175/JCLI3756.1)
- Brohan P, Kennedy JJ, Harris I, Tett SFB, Jones PD (2006) Uncertainty estimates in regional and global observed temperature changes: a new data set from 1850. *J Geophys Res* 111(D12):D12106. doi:[10.1029/2005JD006548](https://doi.org/10.1029/2005JD006548)
- Brovkin V, Bendtsen J, Claussen M, Ganopolski A, Kubatzki C, Petoukhov V, Andreev A (2002) Carbon cycle, vegetation and climate dynamics in the Holocene: experiments with the CLIMBER-2 model. *Global Biogeochem Cycles* 16. doi:[10.1029/2001GB001662](https://doi.org/10.1029/2001GB001662)
- Cai WJ, Cowan T (2007) Trends in Southern Hemisphere circulation in IPCC AR4 models over 1950–99: ozone depletion versus greenhouse forcing. *J Clim* 20:681–693. doi:[10.1175/JCLI4028.1](https://doi.org/10.1175/JCLI4028.1)
- Carsey FD (1980) Microwave observation of the Weddell Polynya. *Mon Weather Rev* 108:2032–2044. doi:[10.1175/1520-0493\(1980\)108<2032:MOOTWP>2.0.CO;2](https://doi.org/10.1175/1520-0493(1980)108<2032:MOOTWP>2.0.CO;2)
- Cavalieri DJ, Parkinson CL, Vinnikov KY (2003) 30-year satellite record reveals contrasting Arctic and Antarctic decadal sea ice variability. *Geophys Res Lett* 30(18):1970. doi:[10.1029/2003GL018931](https://doi.org/10.1029/2003GL018931), doi:[10.1029/2003GL018031](https://doi.org/10.1029/2003GL018031)
- Chapman WL, Walsh JE (2007) A synthesis of Antarctic temperatures. *J Clim* 20:4096–4117. doi:[10.1175/JCLI4236.1](https://doi.org/10.1175/JCLI4236.1)
- Ciasto LM, Thompson DWJ (2007) Observations of large-scale ocean-atmosphere interaction in the Southern Hemisphere. *J Clim* 21:1244–1259. doi:[10.1175/2007JCLI1809.1](https://doi.org/10.1175/2007JCLI1809.1)
- Collins M (2003) Quantitative use of paleo-proxy data in global circulation models. *Geophys Res Abstracts* 5:0114
- Comiso JC (2000) Variability and trends in Antarctic surface temperatures from in situ and satellite infrared measurements. *J Clim* 13(10):1674–1696. doi:[10.1175/1520-0442\(2000\)013<1674:VATIAS>2.0.CO;2](https://doi.org/10.1175/1520-0442(2000)013<1674:VATIAS>2.0.CO;2)
- Comiso JC, Nishio F (2008) Trends in the sea ice cover using enhanced and compatible AMSR-E, SSM/I, and SMMR data. *J Geophys Res* 113:C02S07. doi:[10.1029/2007JC004257](https://doi.org/10.1029/2007JC004257)
- Cotté C, Guinet C (2007) Historical whaling records reveal major regional retreat of Antarctic sea ice. *Deep Sea Res Part I Oceanogr Res Pap* 54:243–252. doi:[10.1016/j.dsr.2006.11.001](https://doi.org/10.1016/j.dsr.2006.11.001)
- Crook JA, Gillett NP, Keeley SPE (2008) Sensitivity of Southern Hemisphere climate to zonal asymmetry in ozone. *Geophys Res Lett* 35:L07806. doi:[10.1029/2007GL032698](https://doi.org/10.1029/2007GL032698)
- Curran MA, van Ommen TD, Morgan VI, Phillips KL, Palmer AS (2003) Ice core evidence for Antarctic sea ice decline since the 1950s. *Science* 232:1203–1206. doi:[10.1126/science.1087888](https://doi.org/10.1126/science.1087888)
- de la Mare WK (1997) Abrupt mid-twentieth-century decline in Antarctic sea-ice extent from whaling records. *Nature* 389:57–60. doi:[10.1038/37956](https://doi.org/10.1038/37956)
- de la Mare WK (2008) Changing in Antarctic sea-ice extent from direct historical observations and whaling records. *Clim Change*
- Driesschaert E, Fichefet T, Goosse H, Huybrechts P, Janssens I, Mouchet A, Munhoven G, Brovkin V, Weber SL (2007) Modeling the influence of Greenland ice sheet melting on the Atlantic meridional overturning circulation during the next millennia. *Geophys Res Lett* 34:L10707. doi:[10.1029/2007GL029516](https://doi.org/10.1029/2007GL029516)
- Fahrbach E, Hoppema M, Rohardt G, Schröder M, Wisotzki A (2004) Decadal-scale variations of water mass properties in the deep Weddell Sea. *Ocean Dyn* 54:77–91. doi:[10.1007/s10236-003-0082-3](https://doi.org/10.1007/s10236-003-0082-3)

- Fahrbach E, Hoppema M, Rohardt G, Schröder M, Wisotzki A (2006) Causes of deep-water variation: comment on the paper by L.H. Smedsrud “Warming of the deep water in the Weddell Sea along the Greenwich meridian: 1977–2001”. *Deep Sea Res Part I Oceanogr Res Pap* 53:574–577. doi:[10.1016/j.dsr.2005.12.003](https://doi.org/10.1016/j.dsr.2005.12.003)
- Forster P, Ramaswamy V, Artaxo P, Bernsten T, Betts R, Fahey DW, Haywood J, Lean J, Lowe DC, Myhre G, Nganga J, Prinn R, Raga G, Schulz M, Van Dorland R (2007) Changes in atmospheric constituents and in radiative forcing. In: Solomon S, Qin D, Manning M, Chen Z, Marquis M, Averyt KB, Tignor M, Miller HL (eds) *Climate change 2007: the physical science basis. Contribution of working group I to the fourth assessment report of the intergovernmental panel on climate change*. Cambridge University Press, Cambridge
- Fyfe JC (2006) Southern Ocean warming due to human influence. *Geophys Res Lett* 33:L19701. doi:[10.1029/2006GL027247](https://doi.org/10.1029/2006GL027247)
- Fyfe JC, Saenko O (2006) Simulated changes in the extratropical southern hemisphere winds and currents. *Geophys Res Lett* 33:L06701. doi:[10.1029/2005GL025332](https://doi.org/10.1029/2005GL025332)
- Gille ST (2002) Warming of the Southern Ocean since the 1950s. *Science* 295:1275–1277. doi:[10.1126/science.1065863](https://doi.org/10.1126/science.1065863)
- Gillett NP, Thompson DWJ (2003) Simulation of recent Southern Hemisphere climate change. *Science* 302(5643):273–275. doi:[10.1126/science.1087440](https://doi.org/10.1126/science.1087440)
- Gleckler PJ, Taylor KE, Doutriaux C (2008) Performance metrics for climate models. *J Geophys Res* 113:D06104. doi:[10.1029/2007JD008972](https://doi.org/10.1029/2007JD008972)
- Gong D, Wang S (1999) Definition of Antarctic oscillation index. *Geophys Res Lett* 26(4):459–462. doi:[10.1029/1999GL900003](https://doi.org/10.1029/1999GL900003)
- Goosse H, Fichefet T (1999) Importance of ice-ocean interactions for the global ocean circulation: a model study. *J Geophys Res* 104:23337–23355. doi:[10.1029/1999JC900215](https://doi.org/10.1029/1999JC900215)
- Goosse H, Renssen H (2001) A two-phase response of Southern Ocean to an increase in greenhouse gas concentrations. *Geophys Res Lett* 28:3469–3473. doi:[10.1029/2001GL013525](https://doi.org/10.1029/2001GL013525)
- Goosse H, Renssen H (2005) A simulated reduction in Antarctic sea-ice area since 1750: implications of the long memory of the ocean. *Int J Clim* 25:569–579. doi:[10.1002/joc.1139](https://doi.org/10.1002/joc.1139)
- Goosse H, Renssen H, Timmermann A, Bradley RS, Mann ME (2006) Using paleoclimate proxy-data to select optimal realisations in an ensemble of simulations of the climate of the past millennium. *Clim Dyn* 27:165–184. doi:[10.1007/s00382-006-0128-6](https://doi.org/10.1007/s00382-006-0128-6)
- Goosse H, Driesschaert E, Fichefet T, Loutre MF (2007) Information on the early Holocene climate constrains the summer sea ice projections for the 21st century. *Clim Past* 3:683–692
- Gordon AL (1978) Deep Antarctic convection West of Maud rise. *J Phys Oceanogr* 8:600–612. doi:[10.1175/1520-0485\(1978\)008<0600:DACWOM>2.0.CO;2](https://doi.org/10.1175/1520-0485(1978)008<0600:DACWOM>2.0.CO;2)
- Gordon AL (1982) Weddell deep water variability. *J Mar Res* 40(suppl):199–217
- Gordon AL (1998) Western Weddell Sea thermohaline circulation stratification. In: *Ocean, ice and atmosphere: interactions at Antarctic Continental Margin, Antar. Res. Ser. 75*, edited by SS Jacobs and R Weiss, 215–240, AGU, Washington, DC
- Gordon AL, Visbeck M, Comiso J (2007) A possible link between the Weddell Polynya and the Southern annular mode. *J Clim* 20:2258–2571. doi:[10.1175/JCLI4046.1](https://doi.org/10.1175/JCLI4046.1)
- Gregory JM (2000) Vertical heat transport in the ocean and their effect on time-dependent climate change. *Clim Dyn* 16:501–515. doi:[10.1007/s003820000059](https://doi.org/10.1007/s003820000059)
- Jacobs SS, Giulivi CF, Mele PA (2002) Freshening of the Ross Sea during the late 20th century. *Science* 297:386–389. doi:[10.1126/science.1069574](https://doi.org/10.1126/science.1069574)
- Jones JM, Widmann M (2003) Instrument- and tree-ring based estimates of the Antarctic oscillation. *J Clim* 16:3511–3524. doi:[10.1175/1520-0442\(2003\)016<3511:IATEOT>2.0.CO;2](https://doi.org/10.1175/1520-0442(2003)016<3511:IATEOT>2.0.CO;2)
- Jones JM, Widmann M (2004) Early peak in Antarctic oscillation index. *Nature* 432:290–291. doi:[10.1038/432290b](https://doi.org/10.1038/432290b)
- Lefebvre W, Goosse H (2008a) Analysis of the projected regional sea-ice changes in the Southern Ocean during the 21st century. *Clim Dyn* 30:59–76. doi:[10.1007/s00382-007-0273-6](https://doi.org/10.1007/s00382-007-0273-6)
- Lefebvre W, Goosse H (2008b) An analysis of the atmospheric processes driving the large-scale winter sea-ice variability in the Southern Ocean. *J Geophys Res* 113:C02004. doi:[10.1029/2006JC004032](https://doi.org/10.1029/2006JC004032)
- Lefebvre W, Goosse H, Timmermann R, Fichefet T (2004) Influence of the southern annular mode on the sea-ice-ocean system. *J Geophys Res* 109:C090005. doi:[10.1029/2004JC002403](https://doi.org/10.1029/2004JC002403)
- Lemke P, Ren J, Alley RB, Allison I, Carrasco J, Flato G, Fujii Y, Kaser G, Mote P, Thomas RH, Zhang T (2007) Observations: changes in snow, ice and frozen ground. In: Solomon S, Qin D, Manning M, Chen Z, Marquis M, Averyt KB, Tignor M, Miller HL (eds) *Climate change 2007: the physical science basis. Contribution of working group I to the fourth assessment report of the intergovernmental panel on climate change*. Cambridge University Press, Cambridge
- Liu J, Curry JA, Martinson DG (2004) Interpretation of recent Antarctic sea ice variability. *Geophys Res Lett* 31:L02205. doi:[10.1029/2003GL018732](https://doi.org/10.1029/2003GL018732)
- Manabe S, Stouffer RJ, Spelman MJ, Bryan K (1991) Transient responses of a coupled atmosphere-ocean model to gradual changes of atmospheric CO₂. I. Annual mean response. *J Clim* 4:785–818. doi:[10.1175/1520-0442\(1991\)004<0785:TROACO>2.0.CO;2](https://doi.org/10.1175/1520-0442(1991)004<0785:TROACO>2.0.CO;2)
- Marshall GJ (2003) Trends in the southern annular mode from observations and reanalyses. *J Clim* 14:4134–4143. doi:[10.1175/1520-0442\(2003\)016<4134:TITSAM>2.0.CO;2](https://doi.org/10.1175/1520-0442(2003)016<4134:TITSAM>2.0.CO;2)
- Marshall GJ (2007) Half-century seasonal relationships between the southern annular mode and Antarctic temperatures. *Int J Clim* 27:373–383. doi:[10.1002/joc.1407](https://doi.org/10.1002/joc.1407)
- Marshall GJ, Orr A, van Lipzig NPM, King JC (2006) The impact of a changing southern hemisphere annular mode on Antarctic Peninsula summer temperatures. *J Clim* 19:5388–5404. doi:[10.1175/JCLI3844.1](https://doi.org/10.1175/JCLI3844.1)
- Meehl GA, Stocker TF, Collins WD, Friedlingstein P, Gaye AT, Gregory JM, Kitoh A, Knutti R, Murphy JM, Noda A, Raper SCB, Watterson IG, Weaver AJ, Zhao ZC (2007) Global climate projections. In: Solomon S, Qin D, Manning M, Chen Z, Marquis M, Averyt KB, Tignor M, Miller HL (eds) *Climate change 2007: the physical science basis. contribution of working group I to the fourth assessment report of the intergovernmental panel on climate change*. Cambridge University Press, Cambridge
- Meredith MP, King JC (2005) Rapid climate change in the ocean west of the Antarctic Peninsula during the second half of the 20th century. *Geophys Res Lett* 32(19):L19604
- Miller RL, Schmidt GA, Shindell DT (2006) Forced annular variations in the 20th century intergovernmental panel on climate change fourth assessment report models. *J Geophys Res* 111(D18):D18101. doi:[10.1029/2005JD006323](https://doi.org/10.1029/2005JD006323)
- Monaghan AJ, Bromwich DH, Chapman W, Comiso JC (2008) Recent variability and trends of Antarctic near-surface temperature. *J Geophys Res* 113:D04105. doi:[10.1029/2007JD009094](https://doi.org/10.1029/2007JD009094)
- Murphy EJ, Clarke A, Symon C, Priddle J (1995) Temporal variation in Antarctic sea-ice: analysis of a long term fast-ice record from the South Orkney Islands. *Deep Sea Res Part I Oceanogr Res Pap* 42:1045–1062. doi:[10.1016/0967-0637\(95\)00057-D](https://doi.org/10.1016/0967-0637(95)00057-D)
- Opsteegh JD, Haarsma RJ, Selten FM, Kattenberg A (1998) ECBILT: a dynamic alternative to mixed boundary conditions in ocean models. *Tellus* 50A:348–367
- Orsi AH, Wiederwohl CL (2008) A recount of Ross Sea waters. *Deep Sea Res Part II Top Stud Oceanogr* (in press)

- Ozsoy-Cicek B, Xie H, Ackley SF, Ye K (2008) Antarctic summer sea ice concentration and extent: comparison of ODEN 2006 ship observations, satellite passive microwave and NIC sea ice charts. *Cryosphere Discuss* 2:623–647
- Parkinson CL, Vinnikov KY, Cavalieri DJ (2006) Evaluation of the simulation of the annual cycle of Arctic and Antarctic sea ice coverages by 11 major global climate models. *J Geophys Res* 111(C7):C07012. doi:[10.1029/2005JC003408](https://doi.org/10.1029/2005JC003408)
- Raphael MN, Holland MM (2005) Twentieth century simulation of the southern hemisphere climate in coupled models. Part 1: large-scale circulation variability. *Clim Dyn* 26:217–228. doi:[10.1007/s00382-005-0082-8](https://doi.org/10.1007/s00382-005-0082-8)
- Rayner NA, Parker DE, Horton EB, Folland CK, Alexander LV, Rowell DP, Kent EC, Kaplan A (2003) Global analyses of sea surface temperature, sea ice, and night marine air temperature since the late nineteenth century. *J Geophys Res* 108(D14):4407. doi:[10.1029/2002JD002670](https://doi.org/10.1029/2002JD002670)
- Rintoul SR (2007) Rapid freshening of Antarctic Bottom Water formed in the Indian and Pacific oceans. *Geophys Res Lett* 34:L06606. doi:[10.1029/2006GL028550](https://doi.org/10.1029/2006GL028550)
- Robertson R, Visbeck M, Gordon AL, Fährbach E (2002) Long-term temperature trends in the deep waters of the Weddell Sea. *Deep Sea Res Part II Top Stud Oceanogr* 49:4791–4806. doi:[10.1016/S0967-0645\(02\)00159-5](https://doi.org/10.1016/S0967-0645(02)00159-5)
- Sarmiento JL, Hughes TMC, Stouffer RJ, Manabe S (1998) Simulated response of the ocean carbon cycle to an anthropogenic climate warming. *Nature* 393:245–249. doi:[10.1038/30455](https://doi.org/10.1038/30455)
- Sen Gupta A, England MH (2006) Coupled ocean-atmosphere-ice response to variations in the southern annular mode. *J Clim* 19:4457–4486. doi:[10.1175/JCLI3843.1](https://doi.org/10.1175/JCLI3843.1)
- Smedsrud LH (2005) Warming of the deep water in the Weddell Sea along the Greenwich meridian: 1977–2001. *Deep Sea Res Part I Oceanogr Res Pap* 52:241–258. doi:[10.1016/j.dsr.2004.10.004](https://doi.org/10.1016/j.dsr.2004.10.004)
- Son SW, Polvani LM, Waugh DW, Akiyoshi H, Garcia R, Kinnison D, Pawson S, Rozanov E, Shepherd TG, Shibata K (2008) The impact of stratospheric ozone recovery on the southern hemisphere westerly jet. *Science* 320:1486–1489. doi:[10.1126/science.1155939](https://doi.org/10.1126/science.1155939)
- Stammerjohn SE, Martinson DG, Smith RC, Yuan X, Rind D (2008) Trends in Antarctic annual sea ice retreat and advance and their relation to El Niño-Southern Oscillation and Southern Annual Mode variability. *J Geophys Res* 113:C03S90. doi:[10.1029/2007JC004269](https://doi.org/10.1029/2007JC004269)
- Steig EJ, Schneider DP, Rutherford SD, Mann ME, Comiso JC, Shindell DT (2008) Warming of the Antarctic ice sheet surface since the 1957 international geophysical year. *Nature* (in press)
- Stover CL (2006) A new account of Ross Sea waters characteristics. Dissertation, Texas A&M University, p 112
- Swingedouw D, Fichefet T, Huybrechts P, Goosse H, Driesschaert E, Loutre MF (2008) Antarctic ice-sheet melting provides negative feedbacks on future climate warming. *Geophys Res Lett* 35:L17705. doi:[10.1029/2008GL034410](https://doi.org/10.1029/2008GL034410)
- Thompson DWJ, Solomon S (2002) Interpretation of Recent southern hemisphere climate change. *Science* 296:895–899. doi:[10.1126/science.1069270](https://doi.org/10.1126/science.1069270)
- Turner J, Colwell SR, Marshall GJ, Lachlan-Cope TA, Carleton AM, Jones PD, Lagun V, Reid PA, Iagovkina S (2005) Antarctic climate change during the last 50 years. *Int J Clim* 25:279–294. doi:[10.1002/joc.1130](https://doi.org/10.1002/joc.1130)
- van Lipzig NPM, Marshall GJ, Orr A, King JC (2008) The relationship between the southern hemisphere annular mode and Antarctic Peninsula temperatures: analysis of a high-resolution model climatology. *J Clim* 21:1649–1668. doi:[10.1175/2007JCLI1695.1](https://doi.org/10.1175/2007JCLI1695.1)
- Vaughan DG, Marshall GJ, Connolley WM, Parkinson C, Mulvaney R, Hodgson DA, King JC, Pudsey CJ, Turner J (2003) Recent rapid regional climate warming on the Antarctic Peninsula. *Clim Change* 60:243–274. doi:[10.1023/A:1026021217991](https://doi.org/10.1023/A:1026021217991)
- Whitworth TIII (2002) Two modes of bottom water in the Australian-Antarctic Basin. *Geophys Res Lett* 29:1073. doi:[10.1029/2001GL014282](https://doi.org/10.1029/2001GL014282)
- Yuan X, Li C (2008) Climate modes in southern high latitudes and their impact on Antarctic sea ice. *J Geophys Res* 113:C06S91. doi:[10.1029/2006JC004067](https://doi.org/10.1029/2006JC004067)
- Zhang J (2007) Increasing Antarctic sea ice under warming atmospheric and oceanic conditions. *J Clim* 20:2515–2529. doi:[10.1175/JCLI4136.1](https://doi.org/10.1175/JCLI4136.1)
- Zwally HJ, Comiso JC, Parkinson CL, Cavalieri DJ, Gloersen P (2002) Variability of Antarctic sea ice 1979–1998. *J Geophys Res* 107(C5). doi:[10.1029/2000JC000733](https://doi.org/10.1029/2000JC000733)